Hexagons and interfaces in a vibrated granular layer

I. S. Aranson,[1] L. S. Tsimring,[2] and V. M. Vinokur[1]
[1]*Argonne National Laboratory, 9700 South Cass Avenue, Argonne, Illinois 60439*
[2]*Institute for Nonlinear Science, University of California, San Diego, La Jolla, California 92093-0402*
(Received 13 February 1998)

The order parameter model based on the parametric Ginzburg-Landau equation is used to describe high acceleration patterns in the vibrated layer of granular material. At large amplitude of driving both hexagons and interfaces emerge. Transverse instability, leading to the formation of ''decorated'' interfaces and labyrinthine patterns, is found. Additional subharmonic forcing leads to controlled interface motion.
[S1063-651X(99)50102-5]

PACS number(s): 47.54.+r, 45.05.+x, 47.35.+i, 83.70.Fn

Driven granular systems manifest collective fluidlike behavior: convection, surface waves, and pattern formation (see, e.g., [1]). One of the most fascinating examples of this collective dynamics is the appearance of long-range coherent patterns and localized excitations in vertically vibrated thin granular layers [2–4]. The particular pattern is determined by the interplay between driving frequency f and acceleration of the container $\Gamma = 4\pi^2 \mathcal{A} f^2/g$ ($\mathcal{A}$ is the amplitude of oscillations, and g is the gravity acceleration) [2,3]. Patterns appear at $\Gamma \approx 2.4$ almost independently of the driving frequency f. At small frequencies $f < f^*$ [5] the transition is subcritical (hysteretic), leading to the formation of squares. In the hysteretic region, localized excitations such as individual *oscillons* and various bound states of oscillons appear as Γ is decreased. For higher frequencies $f > f^*$ the onset pattern is stripes, and at the frequency slightly higher than f^* the transition becomes supercritical. Both squares and stripes, as well as oscillons, oscillate at half of the driving frequency $f/2$. At higher acceleration ($\Gamma > 4$), stripes and squares become unstable, and hexagons appear instead. Further increase of acceleration at $\Gamma \approx 4.5$ converts hexagons into a domainlike structure of flat layers oscillating with frequency $f/2$ with opposite phases. Depending on parameters, interfaces separating flat domains, are either smooth or ''decorated'' by periodic undulations. For $\Gamma > 5.7$ various quarter-harmonic patters emerge.

The pattern formation in thin layers of granular material was studied theoretically by several groups. Direct molecular dynamics simulations [6] (see also [7]) reproduced a majority of patterns observed in experiments and many features of the bifurcation diagram, although until now have not yielded oscillons and interfaces. Hydrodynamic and phenomenological models [8] reproduced certain experimental features; however, neither of them offered a systematic description of the whole rich variety of the observed phenomena. In Ref. [9] we introduced the order parameter characterizing the complex amplitude of subharmonic oscillations. The equations of motion following from the symmetry arguments and mass conservation reproduced essential phenomenology of patterns near the threshold of primary bifurcation: stripes, squares, and oscillons.

In this Rapid Communication we describe high acceleration patterns on the basis of the order parameter model. We show that at large amplitude of driving both hexagons and interfaces emerge. We find morphological instability leading to the formation of ''decorated'' interfaces. Additional subharmonic forcing leads to the motion of the interface with the direction controlled by relative phases of harmonic and subharmonic components of forcing.

The essence of the model [9,10] is the order parameter equation for the complex amplitude ψ of parametric layer oscillations $h = \psi \exp(i\pi f t) + \text{c.c.}$ at the frequency $f/2$ coupled with the the average thickness of the layer ρ. However, at high frequencies ($f > f^*$) the coupling between ρ and ψ becomes less relevant (ρ becomes enslaved by ψ), and the model can be reduced to a single order-parameter equation

$$\partial_t \psi = \gamma \psi^* - (1 - i\omega)\psi + (1 + ib)\nabla^2 \psi - |\psi|^2 \psi. \qquad (1)$$

Equation (1) describes the evolution of the order parameter for the parametric instability in spatially extended systems (see [11,12]). Linear terms in this equation are obtained from the complex growth rate for infinitesimal periodic layer perturbations $h \sim \exp[\Lambda(k)t + ikx]$. Expanding $\Lambda(k)$ for small k, and keeping only two leading terms in the expansion $\Lambda(k) = -\Lambda_0 - \Lambda_1 k^2$ we obtain the linear terms in Eq. (1), where $b = \mathrm{Im}\,\Lambda_1/\mathrm{Re}\,\Lambda_1$ and $\omega = (\Omega_0 - \pi f)/\mathrm{Re}\,\Lambda_0$, where $\Omega_0 = -\mathrm{Im}\,\Lambda_0$. The term $\gamma\psi^*$ characterizes the effect of driving at the resonance frequency. The term $-|\psi|^2\psi$ accounts for nonlinear saturation of waves at finite amplitude.

It is convenient to shift the phase of the complex order parameter via $\tilde{\psi} = \psi \exp(i\phi)$ with $\sin 2\phi = \omega/\gamma$. The equations for real and imaginary part $\tilde{\psi} = A + iB$ are

$$\partial_t A = (s-1)A - 2\omega B - (A^2 + B^2)A + \nabla^2(A - bB), \qquad (2)$$

$$\partial_t B = -(s+1)B - (A^2 + B^2)B + \nabla^2(B + bA), \qquad (3)$$

where $s^2 = \gamma^2 - \omega^2$. At $s < 1$, Eqs. (2) and (3) have only one trivial uniform state $A = 0$, $B = 0$. At $s > 1$, two new uniform states appear: $A = \pm A_0, B = 0, A_0 = \sqrt{s-1}$. The onset of these states corresponds to the period doubling of the layer flights sequence, observed in experiments [2] and predicted by the simple inelastic ball model [2,13]. Signs $\pm$ reflect two relative phases of layer flights with respect to container vibrations.

First we analyze the stability of the state $A = \pm A_0, B = 0$ with respect to perturbations with wave number k, (A,B)

$=(A_0,0)+(U_k,V_k)\exp[\lambda(k)t+ikx]$. The uniform state loses its stability with respect to periodic modulations with the wave number k_c at $s<s_c$ (correspondingly, $\gamma<\gamma_c$), where

$$s_c=\frac{\sqrt{(1+\omega^2)(1+b^2)}-\omega+b}{2b}, \tag{4}$$

$$k_c^2=-\frac{2s-1-\omega b}{1+b^2}. \tag{5}$$

Small perturbations with all directions of the wave vector grow with the same rate. The resultant selected pattern is determined by the nonlinear competition between the modes. In the presence of the reflection symmetry $\psi\to-\psi$, quadratic nonlinearity is absent, and cubic nonlinearity favors stripes corresponding to a single mode. Near the fixed points $A=A_0,B=0$ the reflection symmetry for perturbations $U\to-U,V\to-V$ is broken, and hexagons emerge at the threshold of instability. To clarify this point we perform weakly nonlinear analysis of Eqs. (2) and (3) for $s=s_c-\epsilon$, and $\epsilon\ll1$. At $\epsilon\to0$, the variables U and V are related as in linear system,

$$(U,V)=(1,\eta)\Psi,\quad \eta=[2(s_c-1)+k_c^2]/(bk_c^2-2\omega), \tag{6}$$

$$\Psi=\sum A_j\exp[i\mathbf{k}\cdot\mathbf{r}]+\text{c.c.},\quad |k|=k_c.$$

The corresponding adjoint eigenvector is

$$(U^+,V^+)=(1,\eta^+),\quad \eta^+=-[2(s_c-1)+k_c^2]/bk_c^2. \tag{7}$$

Substituting Eq. (6) into Eqs. (2) and (3) and performing the orthogonalization, we obtain equations for the slowly varying complex amplitudes A_j, $j=1,2,3$ (we assume only three waves with triangular symmetry, favored by quadratic nonlinearity),

$$\partial_t A_j=2\epsilon A_j+a_2A_{j+1}^*A_{j-1}^*-a_3[|A_j|^2+2(|A_{j-1}|^2+|A_{j+1}|^2)]A_j, \tag{8}$$

where the coefficients a_2,a_3 are

$$a_2=2A_0\left(2+\frac{1+\eta^2}{1+\eta\eta^+}\right),\quad a_3=3(1+\eta\eta^+). \tag{9}$$

Equations (8) are well-studied (see [14]). There are three critical values of ϵ: $\epsilon_A=-a_2^2/40a_3$, $\epsilon_R=a_2^2/2a_3$, and $\epsilon_B=2a_2^2/a_3$. The hexagons are stable for $\epsilon_A<\epsilon<\epsilon_B$, and the stripes are stable for $\epsilon>\epsilon_R$. Thus, near $s=s_c$ the model exhibits stable hexagons [15]. Since we have two symmetric fixed points, both up- and down-hexagons coexist. For smaller s stripes are stable, and for larger s, flat layers are stable, in agreement with observations [3,19]. The above analysis requires the values of $\epsilon_{A,B,R}$ to be small. For parameters $\omega,b=O(1)$, this requirement is satisfied for ϵ_A, but not for $\epsilon_{B,R}$. The estimates can be improved by substituting A_0 at $s=s_c+\epsilon$ instead of $A_0(s_c)$ in Eq. (9). The resulting range of stable hexagons is plotted in the phase diagram (ω,γ) (see Fig. 1).

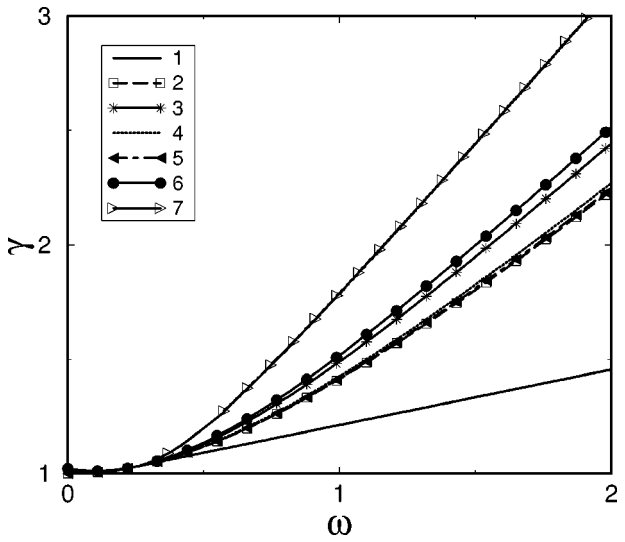

FIG. 1. Phase diagram for Eq. (1) at $b=4$. Line 1, $\gamma^2=(\omega+b)^2/(1+b^2)$; line 2, $s^2\equiv\gamma^2-\omega^2=1$; line 3, $s=s_c$; line 4, $s=s_c-\epsilon_R$; line 5, $s=s_c-\epsilon_B$; line 6, $s=s_c-\epsilon_A$; line 7, $\beta=-1$. Beneath line 1 there are no patterns, between lines 1 and 4 stripes are stable, between lines 5 and 6 hexagons are stable, above line 2 nontrivial flat states exist, and above line 3 they are stable. Interfaces are unstable below line 7.

At $s>1$, Eqs. (2) and (3) have an interface solution connecting two uniform states $A=\pm A_0$, $B=0$. For $b=0$ this solution is of the form $\overline{A}=\pm A_0\tanh(A_0x/2)$, $B=0$. For $b\neq0$ the solution is available only numerically. In order to investigate the stability of the interface, we consider the perturbed solution $(A,B)=(\overline{A},\overline{B})+[\tilde{A}(x),\tilde{B}(x)]\exp[\lambda(k)t+iky]$. For $\tilde{A},\tilde{B}$ we obtain linear equations

$$\hat{L}\begin{pmatrix}\tilde{A}\\ \tilde{B}\end{pmatrix}=[\lambda(k)+k^2]\begin{pmatrix}\tilde{A}\\ \tilde{B}\end{pmatrix}+bk^2\begin{pmatrix}\tilde{B}\\ -\tilde{A}\end{pmatrix},$$

$$\hat{L}=\begin{pmatrix}s-1-3\overline{A}^2-\overline{B}^2+\partial_x^2, & -2\omega-2\overline{AB}-b\partial_x^2\\ -2\overline{AB}+b\partial_x^2, & -s-1-\overline{A}^2-3\overline{B}^2+\partial_x^2\end{pmatrix}. \tag{10}$$

In order to determine the spectrum of eigenvalues $\lambda(k)$ one has to solve Eq. (10) along with stationary Eqs. (2) and (3). Using the numerical matching-shooting technique, we have obtained positive eigenvalues corresponding to interface instability. This instability is confirmed by direct numerical simulations of Eq. (1). An example of the evolution of slightly perturbed interface is shown in Fig. 2. Small perturbations grow to form a ''decorated'' interface similar to [20], with time these decorations evolve slowly and eventually form a labyrinthine pattern.

The neutral curve for this instability can be determined as follows. Numerical analysis shows that at the threshold the most unstable wave number is $k=0$ and we can expect that for $k\to0$ $\lambda\sim k^2$. Expanding Eqs. (10) in power series of k^2: $(\tilde{A},\tilde{B})=(A^{(0)},B^{(0)})+k^2(A^{(1)},B^{(1)})+\cdots$ in the zeroth order in k we obtain $\hat{L}(A^{(0)},B^{(0)})=0$. The corresponding solution is the translation mode $A^{(0)}=\partial_x\overline{A}(x)$, $B^{(0)}=\partial_x\overline{B}(x)$. In the first order in k^2 we arrive at the linear inhomogeneous problem

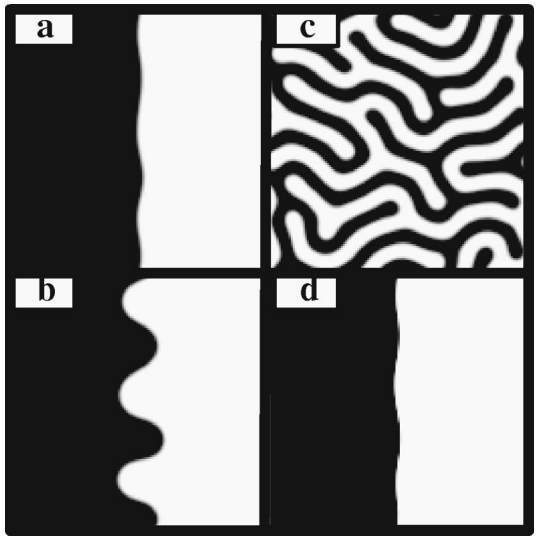

FIG. 2. (a)–(c) Represent interface instability and labyrinth formation, Eq. (1), $\omega=2$, $b=4$, and $\gamma=2.9$, domain size 100×100 units, the snapshots are taken at times $t=1000$, 1600, 4640; (d) represents the stationary decorated interface, $\omega=6$, $b=4$, $\gamma=7.4$, and $\alpha=0.2$; $t=10\,000$.

$$\hat{L}\begin{pmatrix}A^{(1)}\\B^{(1)}\end{pmatrix}=[\lambda(k)+k^2]\begin{pmatrix}A^{(0)}\\B^{(0)}\end{pmatrix}+bk^2\begin{pmatrix}B^{(0)}\\-A^{(0)}\end{pmatrix}. \quad (11)$$

A bounded solution to Eq. (11) exists if the rhs is orthogonal to the localized mode of the adjoint operator A^+,B^+. The orthogonality condition fixes the relation between λ and k,

$$\lambda=-(1+\beta)k^2, \quad \beta=\frac{b\int_{-\infty}^{\infty}(A^{(0)}B^+-B^{(0)}A^+)dx}{\int_{-\infty}^{\infty}(A^{(0)}A^++B^{(0)}B^+)dx}. \quad (12)$$

The instability, corresponding to the negative surface tension of the interface, onsets at $\beta=-1$. The neutral curve is shown in Fig. 1. This instability leads to the so called decorated interfaces see [Fig. 2(a)]. At the nonlinear stage the undulations grow and form labyrinthine patterns [Fig. 2(b)–(d)].

Near the line $s=1$ (see Fig. 1), Eq. (1) can be simplified. In the vicinity of this line $A\sim(s-1)^{1/2}$ and $B\sim(s-1)^{3/2}\ll A$. In the leading order we can obtain from Eq. (3) $B=b\nabla^2A/2$, and Eq. (2) yields [21]

$$\partial_tA=(s-1)A-A^3+(1-\omega b)\nabla^2A-\frac{b^2}{2}\nabla^4A. \quad (13)$$

Rescaling the variables $t\to(s-1)t, A\to(s-1)^{-1/2}A, x\to[2(s-1)/b^2]^{1/4}$, we can reduce Eq. (1) to the Swift-Hohenberg equation (SHE)

$$\partial_tA=A-A^3-\delta\nabla^2A-\nabla^4A, \quad (14)$$

where $\delta=(\omega b-1)\sqrt{2/[(s-1)b^2]}$. This equation is simpler than Eq. (1); however, it captures many essential features of the original system dynamics, including the existence and stability of stripes and hexagons in different parameter regions (see [16]), existence of the interface solutions, interface instability, and the emergence of labyrinthine patterns. Indeed, a simple analysis shows that the growth rate of the instability of the uniform state $A=1$ as a function of the perturbation wave number is determined by the formula $\lambda(k)=-2+\delta k^2-k^4$, so it becomes unstable at $\delta>\delta_c=2\sqrt{2}$ at critical wave number $k_c=\sqrt{2}$. As in the original model, near the threshold of this instability, subcritical hexagonal patterns are preferred. Interface stability can also be analyzed more simply as the linearized operator corresponding to the model (14) is self-adjoint. The threshold value $\delta_{\rm th}=1.011$ is obtained from the following solvability condition:

$$\int_{-\infty}^{\infty}(\delta_{\rm th}A_{0x}^2-2A_{0xx}^2)dx=0. \quad (15)$$

In experiments, the interface instability usually saturates and yields periodic undulations of the interface instead of labyrinthine patterns.

Let us now discuss some possible mechanisms for saturation of ''labyrinthine'' instability of the interface, which is not captured by Eq. (1) [17]. The reason for the proliferation of the labyrinthine pattern is that the flat state is less ''stable'' than the large-amplitude stripe state, and these stripes (produced by the interface instability) invade uniform domains [18]. In real systems, this does not occur because at large amplitude of driving, the relative velocity of layer and the plate at collision becomes small and cellular patterns do not form. Within our order parameter model, this effect can be described by additional higher order nonlinear terms. They can provide additional stabilization of the flat state against the stripe state even in the regime of interface instability. This effect can provide saturation of the interface instability. We examined this hypothesis numerically in the framework of Eq. (1) [and, correspondingly, Eq. (14)] with additional higher order nonlinear term $-\alpha|\Delta\psi|^2\psi$ in the right-hand side. This additional term does not affect flat states but provides additional dissipation for the patterned state. We have indeed found stable decorated interfaces above some critical value of α [see Fig. 2(d)]. Certainly, the specific choice of the higher order term cannot be justified in the framework of phenomenological theory, however we consider this result rather general and useful for understanding of the saturation effect.

In the region of stability ($\beta>-1$) for the original model Eq. (1) the interface is stationary due to symmetry. However, if the plate oscillates with two frequencies, f and $f/2$, the symmetry between two states connected by the interface, is broken, and interface moves. The velocity of interface motion depends on the relative phase of the subharmonic forcing with respect to the forcing at f. This effect can be described by the additional term $qe^{i\Phi}$ in Eq. (1), where q characterizes the amplitude of the subharmonic pumping, and Φ determines its relative phase. For small q, we look for moving interface solution in the form $\psi=\psi_0(x-vt)+q\psi_1(x-vt)+\cdots$ and $v=O(q)$. Solvability condition yields the following expression for the interface velocity

$$v=-q\frac{\cos\Phi\int A^+dx+\sin\Phi\int B^+dx}{\int(A^+\partial_xA_0+B^+\partial_xB_0)dx}. \quad (16)$$

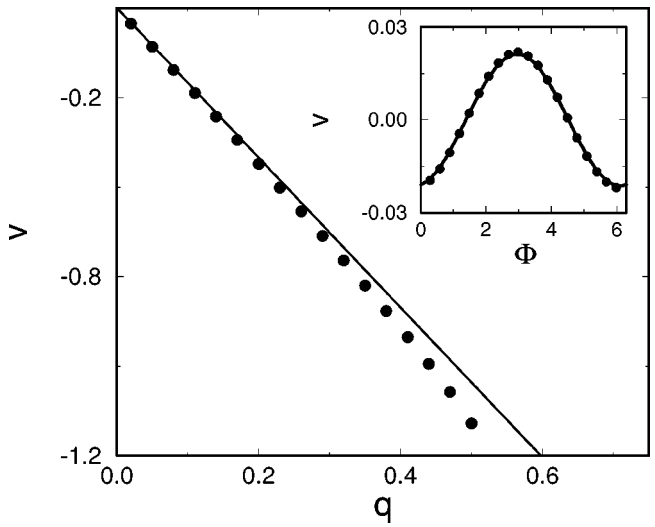

FIG. 3. Interface velocity v for $\omega=1, b=4, \gamma=2.5$ vs q at $\Phi=0$. Inset: v vs Φ at $q=0.01$. (●), numerical results; (—), analytical expression (16).

The explicit answer is possible to obtain for $b=0$ when $A^+=\partial_x A_0$, and $\Phi=0,\pi$, which yields the interface velocity $v=\mp\frac{3}{2}qA_0^{-2}=\mp\frac{3}{2}q(s-1)^{-1}$. In general, A, B, A^+, B^+, and hence v, can be found numerically. The interface velocity as function of q,Φ is shown in Fig. 3.

We have shown that large acceleration patterns are captured by the generic parametric Ginzburg-Landau equation (1). The structure of the phase diagram Fig. 1 is qualitatively similar to that of experiments Refs. [2,19,20] for high frequencies of vibration. Increasing vibration amplitude leads to transition from a trivial state to stripes, hexagons, decorated interfaces, and finally, to stable interfaces. In experiments, at yet higher Γ, quarter-harmonic patterns appear; however, these patterns are not described by our model. The transition from unstable to stable interfaces also occurs with decreasing ω (increasing vibration frequency f), in agreement with Refs. [19,20]. In our original model, the interface instability leads to labyrinthine patterns; however, in experiments this instability usually saturates to provide stationary ''decorations.'' We showed that this saturation may be caused by certain higher order nonlinear terms that suppress stripe formation at large Γ. For additional subharmonic driving the model predicts steady moving interfaces with the direction of motion controlled by the phase of the subharmonic component. Experimental study of the controlled interface motion will be reported elsewhere [22].

We acknowledge useful discussions with R. Behringer, J. de Bruyn, R. Goldstein, H. Jaeger, and H. Swinney. This work was supported by the U.S. DOE under Grant Nos. DE-FG03-95ER14516, DE-FG03-96ER14592, and W-31-109-ENG-38, and by the NSF, under Contract No. STCS #DMR91-20000.

[1] H. M. Jaeger, S. R. Nagel, and R. P. Behringer, Phys. Today **49**(4), 32 (1996); Rev. Mod. Phys. **68**, 1259 (1996).
[2] F. Melo, P. Umbanhowar, and H. L. Swinney, Phys. Rev. Lett. **72**, 172 (1994); **75**, 3838 (1995)
[3] P. B. Umbanhowar, F. Melo, and H. L. Swinney, Nature (London) **382**, 793 (1996).
[4] T. H. Metcalf, J. B. Knight, and H. M. Jaeger, Physica A **236**, 202 (1997).
[5] In experiments [2,3] $f^*\approx 40$ Hz.
[6] C. Bizon *et al.*, Phys. Rev. Lett. **80**, 57 (1998).
[7] S. Luding *et al.*, Europhys. Lett. **36**, 247 (1996).
[8] D. Rothman, Phys. Rev. E **57**, 1239 (1998); E. Cerda, F. Melo, and S. Rica, Phys. Rev. Lett. **79**, 4570 (1997); T. Shinbrot, Nature (London) **389**, 574 (1997); S. C. Venkataramani and E. Ott, Phys. Rev. Lett. **80**, 3495 (1998); J. Eggers and H. Riecke, e-print patt-sol/9801004.
[9] L. S. Tsimring and I. S. Aranson, Phys. Rev. Lett. **79**, 213 (1997).
[10] I. S. Aranson and L. T. Tsimring, Physica A **249**, 103 (1998).
[11] W. Zhang and J. Vinals, Phys. Rev. Lett. **74**, 690 (1995).
[12] S. V. Kiyashko *et al.*, Phys. Rev. E **54**, 5037 (1996).
[13] A. Mehta and J. M. Luck, Phys. Rev. Lett. **65**, 393 (1990).
[14] M. Cross and P. C. Hohenberg, Rev. Mod. Phys. **65**, 851 (1993).
[15] This analysis is similar to that of Ref. [16], where stability of hexagons was demonstrated for the SHE. In a certain limit Eq. (1) can be reduced to SHE (see below).
[16] G. Dewel *et al.*, Phys. Rev. Lett. **74**, 4647 (1995).
[17] We observed the formation of labyrinthinelike patterns in a relatively narrow region of the parameters close to the interface instability line in experiments with particles with substantial wet (oil) coating.
[18] We consider competition between the flat state $\psi=\pm A_0$ and large-amplitude stripe patterns with zero mean, which can be approximated as periodic bound state of the interfaces. Small amplitude stripes bifurcating from flat state (i.e., having nonzero mean close to A_0) are unstable in this region of parameters.
[19] P. K. Das and D. Blair, Phys. Lett. A **242**, 326 (1998).
[20] P. B. Umbanhowar, Ph.D. thesis, University of Texas, Austin, 1996 (unpublished).
[21] SHE for oscillatory systems with strong resonance coupling was derived by P. Coullet and K. Emilson, Physica D **61**, 119 (1992).
[22] I. Aranson *et al.*, Phys. Rev. Lett. (to be published).